Heliyon 10 (2024) e34012

Contents lists available at ScienceDirect

Heliyon

journal homepage: www.cell.com/heliyon

Research article

Constructing an immune-related prognostic signature for predicting prognosis and immune response in hepatocellular carcinoma

Lichao Cao [a,1], Deliang Huang [b,1], Shenrui Zhang [a], Zhiwei Li [b], Qingxian Cai [b], Fang Chen [a], Meilan Zhu [a], Ying Ba [a], Jun Chen [b,**], Hezi Zhang [a,*]

[a] Shenzhen Nucleus Gene Technology Co., Ltd., 518071, Shenzhen, Guangdong Province, China
[b] Department of Liver Diseases, The Third People's Hospital of Shenzhen, The Second Affiliated Hospital of Southern University of Science and Technology, 518100, Shenzhen, Guangdong Province, China

ARTICLE INFO

Keywords:
Hepatocellular carcinoma
Tumor immune microenvironment
Prognosis
Immunotherapy

ABSTRACT

Background: Currently, there are few studies on immune-related prognostic analysis of hepatocellular carcinoma (HCC). Our aim was to establish an immune-correlated prognostic model for HCC.

Methods: Immune-associated cells were obtained from the scRNA-seq dataset (GSE149614) of HCC. Differentially expressed genes between normal and tumor cells from immune-associated cells and the immune-related genes from the ImmPort database were used to identify immune-related differentially expressed genes (IRDEGs). Subsequently, the risk model was established in the TCGA-LIHC cohort (n = 438) from the Cancer Genome Atlas (TCGA) database by using Kaplan-Meier (K-M) survival curve, univariate/multivariate Cox regression analysis. Subsequently, we further analyzed tumor immune microenvironment characteristics, somatic mutation, immune checkpoint and its ligand expression levels between high- and low-risk groups, as well as drug sensitivity prediction. ICGC cohort was set as the validation cohort. TCGA-LIHC cohort and three independent the Gene Expression Omnibus (GEO) datasets (GSE54236, GSE14520, and GSE64041) was used to verify IRDEGs expression, as well as PCR assays using clinical samples.

Results: The IRDEGs was composed of 4 genes, namely B2M, SPP1, PPIA, and HRG. The 438 HCC patients were divided into high- and low-risk group. The high-risk group was associated with poor prognosis, including higher T stage, advanced pathological stages, less immune cell infiltration, higher TP53 mutation rate, the high expression of CTLA4 and HAVCR2. Besides, high-risk populations benefit from most chemotherapy drugs. Similarly, the performance of the risk model was validated in the ICGC. All four datasets (TCGA-LIHC cohort, GSE54236, GSE14520, and GSE64041) and clinical q-PCR results demonstrated that, compared with normal samples, the expressions of B2M and HRG were lower in tumor samples, and the expression of SPP1 was higher.

Conclusion: In summary, the immune-related prognostic signature had a good predictive performance on prognosis and immunotherapy for HCC patients.

* Corresponding author.
** Corresponding author.
E-mail addresses: drchenjun@163.com (J. Chen), hezizhang2020@163.com (H. Zhang).
[1] Lichao Cao and Deliang Huang contributed equally to this work.

https://doi.org/10.1016/j.heliyon.2024.e34012
Received 14 March 2024; Received in revised form 6 June 2024; Accepted 2 July 2024
Available online 3 July 2024

1. Introduction

Liver malignancies remain a global health threat, with the number of cases expected to exceed one million by 2025 [1]. Hepatocellular carcinoma (HCC) is common malignant tumor of the liver, accounting for over 80 % of all primary liver cancers [2]. It is estimated that 1.3 million people are expected to die from liver cancer by 2040 (an increase of 56.4 % from 2020) [3]. Clinically, the effective treatment options for HCC are percutaneous approach, liver transplantation, hepatectomy, etc. [4,5], but the overall prognosis (OS) remains poor. The tumor microenvironment (TME) is important for the recurrence susceptibility and drug resistance of HCC [6,7]. Hence, to better improve the prognosis of HCC patients, it is meaningful to elucidate the relationship between the TME and HCC, resulting in establishing a reliable prognostic model for HCC.

Currently, immunotherapy has been proven effective and safe in treatment of solid tumors [8], among which immune checkpoint inhibitors (ICIs), adoptive cell therapy, and tumor vaccines are common tumor immunotherapy methods in clinical practice. For instance, the U.S. Food and Drug Administration authorized Nivolumab as the first programmed death-1 (PD-1) inhibitor for HCC treatment [9,10]. Moreover, adoptive T-cell therapy represented a promising therapeutic approach for HBV-associated HCC [11]. However, the aboved immunotherapy is only effective for a small percentage of HCC patients and lacks sensitivity for most patients [12].

The TME of HCC is a complex structural hybrid that coexists and interacts with multiple immune cells to impact the efficacy of immunotherapy, leading to sustain HCC development [13]. T cells are the pivotal immune cells in the anti-tumor immune response, which can kill tumor cells in an antigen-specific manner [14]. In addition, natural killer (NK) cells are cytotoxic lymphocytes of the innate immune system, capable of killing cancer cells [15]. In tumor immunity, T cells and NK cells have complementary roles by sharing several important inhibitory and activating receptors that target enhancement of T cells- and NK cells-mediated immune responses [16]. Besides, as one of the most important immune cells, B cells play a key role in both innate and adaptive immunity. According to research findings, the co-presence of $CD8^+$ T cells and $CD20^+$ B cells in tumor tissue was associated with better prognosis in patients with metastatic melanoma [17]. Therefore, elucidating the crosstalk of the TME and immune cells is critical to help formulate personalized immunotherapeutic strategies for HCC patients.

Here, we developed an immune prognostic model for HCC, with a view to providing reference for predicting immunotherapy and prognosis in HCC patients.

2. Materials and methods

2.1. Data download and processing

Fig. 1 has shown the analysis route. The Gene Expression Omnibus (GEO) database (https://www.ncbi.nlm.nih.gov/geo/) has offered the single-cell RNA-seq (scRNA-seq) dataset (GSE149614). A total of 63,101 cells were acquired in GSE149614, including 28,687 normal cells and 34,414 tumor cells. We then selected immune cells (T, B, and NK cells) for follow-up analysis based on the

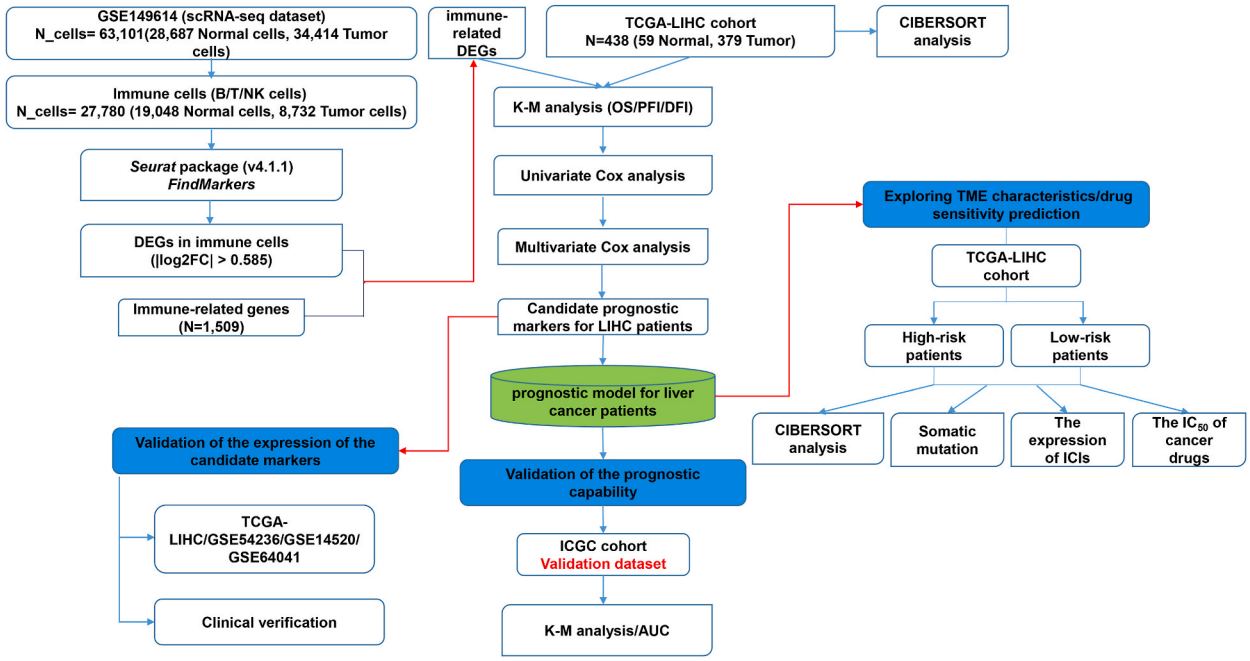

Fig. 1. The flow chart of our study.

isolated cell cluster information reported by Lu et al. [18].

Immune-associated genes were from the ImmPort database (https://immport.niaid.nih.gov/).

TCGA-LIHC cohort (https://xenabrowser.net/datapages/) has offered a total of 438 HCC samples, including the transcriptome data, clinical information, survival information, somatic mutation data. Next, the samples (n = 438) were divided into the normal group (n = 59) and tumor group (n = 379). See Table S1 for detailed information.

The ICGC (https://dcc.icgc.org/) dataset was used to verify the prognostic value, including the transcriptome, clinical and survival data.

Three independent datasets (GSE54236, GSE14520, and GSE64041) were used for validation. GSE54236 included 161 HCC samples, GSE14520 included 488 HCC samples, and GSE64041 included 125 HCC samples.

2.2. Identification of immune-related differentially expressed genes

The Seurat package (v.4.1.1) in the R package (v.4.0.2) was performed to analyze the scRNA-seq data. Filter criteria refer to our previous report [19]. Subsequently, we used the FindMarkers function (logfc.threshold = 0.585) to identify differentially expressed genes (DEGs) between tumor and normal cells in selected immune cells. The immune-related DEGs (IRDEGs) were obtained by taking the intersection of DEG and immune-related genes.

2.3. Generation of the immune-related risk model in HCC

Kaplan-Meier (K-M) survival curve was used to identify the relationship between IRDEGs and the progression free interval (PFI), OS, and disease free interval (DFI) of HCC patients. The candidate prognostic genes were identified by overlapping the factors with $P < 0.05$ in three K-M survival curves. Then, the univariate and multivariate Cox regression models and the survival R package were used to obtain optimal IRDEGs with prognostic ability. K-M curves described the survival of each group in the risk model. The predictive power of the model was evaluated using receiver operating characteristic curve (ROC). Moreover, we investigated the relationship between immune-related risk model and clinical and pathological features using Wilcoxon tests.

2.4. Evaluation the associations between the risk model and immune cell infiltration, mutation profiles and clinical treatments

The TCGA-LIHC cohort was grouped into high- and low-risk groups. CIBERSORT algorithm was performed to obtain the proportion of tumor-infiltrating immune cells [20]. The unpaired *t*-test was performed to compare the levels of immune cells between the two groups. K-M curve was applied to further evaluate the relationship between OS and immune cell with (*P*-value <0.05). The maftools R package was performed to calculate and visualized the mutation profiles [21]. Similarly, K-M method was used to calculate the OS, and the Wilcoxon test was used to compare the expression of immune checkpoint molecules between different groups. Moreover, *oncoPredict* R package [22] was used to predict the maximal IC_{50} of the two groups.

2.5. Verification of the model performance in ICGC cohort and IRDEGs expression in multiple cohorts and clinical samples

The signature of the risk model was validated in the ICGC cohort by using K-M method and ROC curve. The Kruskal-Wallis test was applied to text the expression of 4-IRDEGs in the TCGA-LIHC, GSE54236, GSE14520, and GSE64041.

Six HCC patients were recruited from October 2023 to December 2023 at the Third People's Hospital of Shenzhen. The tumor and para-cancerous tissues were obtained during the operation for q-PCR assay. Total RNA was extracted by TRIzol reagent (TIANGEN, Beijing, China), and was used to cDNA by Hifair® III 1st Strand cDNA Synthesis SuperMix for qPCR (gDNA digester plus) (Yesen, Shanghai, China). Hieff® qPCR SYBR Green Master Mix (No Rox) (Yesen, Shanghai, China) was used for the q-PCR. Relative quantification was determined using the $2^{-\Delta\Delta Ct}$ method. The primers were shown in Table S2. The study was approved by the Ethics Committee of Third People's Hospital of Shenzhen (No. 2022-068). All participants provided written informed consent to participate in this study and for their data to be published.

2.6. Statistical analysis

The mean ± standard error of mean (SEM) was used to show the data. Graph Pad 8.0 was utilized to analyze. The Student's *t*-test was applied to compare continuous variables between the two groups. $P < 0.05$ was considered significant.

3. Results

3.1. Construction of immune-related risk assessment model

A total of 27,780 immune cells (T/B/NK cells) were isolated from a single-cell atlas of the multicellular ecosystem of HCC [18], and after rigorous quality control, a total of 27,586 high-quality immune cells were analyzed (Fig. 2A). Subsequently, we identified 439 DEGs between tumor and normal cells in selected immune cells. Next, 1509 immune-related genes were downloaded from ImmPort database. By overlapping the immune-related genes and DEGs of immune cells, we identified 52 IRDEGs for subsequent analysis (Fig. 2B).

Based on the TCGA-LIHC cohort, we established the immune-associated prognostic model. The K-M analysis (PFI/OS/DFI) was performed to screen the potential prognostic signatures. As shown in Figs. S1A–C, there were 6 common IRDEGs (APOH, B2M, HRG, KNG1, PPIA, and SPP1) had the prognostic ability in different survival curves ($P < 0.05$). Next, the univariate (Table 1) and multivariate Cox regression (Fig. 3A) analyses of PFI were applied on the IRDEGs, and the 4 IRDEGs (B2M, SPP1, PPIA, and HRG) were finally considered as optimal immune genes with prognostic ability. Then, K-M analysis showed that the high-risk group had the worse survival outcomes ($P < 0.0001$, Fig. 3B). In addition, the ROC curve also varies with time (Fig. 3C). Similarly, the OS and DFI associated univariate and multivariate Cox regression analyses (Fig. 3D and G), the K-M survival analysis (Fig. 3E and H) and time-dependent ROC analysis (Fig. 3F and I) were validated the predictive efficacy of the 4-IRDEGs signature.

3.2. Correlation between the risk model and the clinicopathologic features in HCC patients

The correlation between 4 IRDEGs and tumor staging was analyzed, respectively. As exhibited in Fig. 4A and B, the risk score was associated with clinical stage and T stage based on patients' PFI statistics. Similarly, based on patients' OS and DFI information, the risk score was closely associated with clinical stage and T stage, which can predict patients' tumor stage (Fig. 4C–F). These findings demonstrated that the 4-IRDEGs signature has excellent potential to predict HCC patient's prognosis by evaluating their risk score.

3.3. Exploring the immune cell infiltration and mutation profile of the prognostic signature

We evaluated the relationship between the immune cell infiltration level and the risk score in the TCGA-LIHC cohort using the CIBERSORT method. As shown in Fig. 5A, the follicular helper T cells, regulatory T cells, γ-δ T cells, resting NK cells, monocytes, M0 and M2 macrophages, resting dendritic cells, activated mast cells and neutrophils showed significant differences between the normal and tumor groups. Moreover, there were remarkable differences in naive B cells, $CD8^+$ T cells, follicular helper T cells, regulatory T cells, γ-δ T cells, M0 and M1 macrophages, resting mast cells, and eosinophils between the high- and low-risk groups (Fig. 5B). The K-M curve showed that high level of $CD8^+$ T cells had significantly better OS than low level of $CD8^+$ T cells ($P = 0.027$, Fig. 5C). Genes such as TP53, TTN, CTNNB1, MUC16, PCLO, ALB, MUC4, ABCA13, APOB, RYR2, LRP1B, OBSCN, CSMD3, XIRP2, AXIN1, FLG, CACNA1E, HMCN1, RYR1, SPTA1 were top 20 significantly mutated genes in tumors (Fig. 5D). MUC16 showed high mutation rates in the low-risk group (20 % vs. 13 %), and TP53 showed higher mutation rates in the high-risk group (34 % vs. 23 %) (Fig. 5E). Unsurprisingly, there was a remarkable relationship between the mutation status of TP53 and HCC patients' OS ($P = 0.0197$, Fig. 5F). These results indicated TME and gene mutation were important for the development and prognosis of HCC.

3.4. Study of clinical treatment with the risk model

To investigate whether the prognostic model is concerned with immunosuppressive point biomarkers, the Wilcoxon test was applied to compare the expressions of immune checkpoint-related genes in the two groups. The results suggested that high expression of CTLA4 ($P = 0.01$, Fig. 6A) and HAVCR2 ($P = 0.0034$, Fig. 6B) were was positively correlated with the high-risk group, and PD-L1 presented with high expression in the low-risk group ($P = 0.0062$, Fig. 6C). However, PD-1 ($P = 0.16$, Fig. 6D), TIGIT ($P = 0.79$, Fig. 6E), and LAG-3 ($P = 0.13$, Fig. 6F) expression levels were not significantly different. Moreover, chemotherapeutics also played a vital role in treating HCC patients. Drug sensitivity analysis indicated that vinblastine, staurosporine, pictilisib, paclitaxel, and trametinib might be more effective in high-risk patients, while rapamycin and bortezomib-1191 might be more effective for low-risk patients (Fig. 6G). Moreover, we predicted the IC_{50} values of 6 drugs commonly used in HCC. The results showed the IC_{50} value of Lapatinib was lower in the high-risk group (Fig. S2A), while the IC_{50} values of Camptothecin, Cytarabine, Docetaxel, Gemcitabine, and

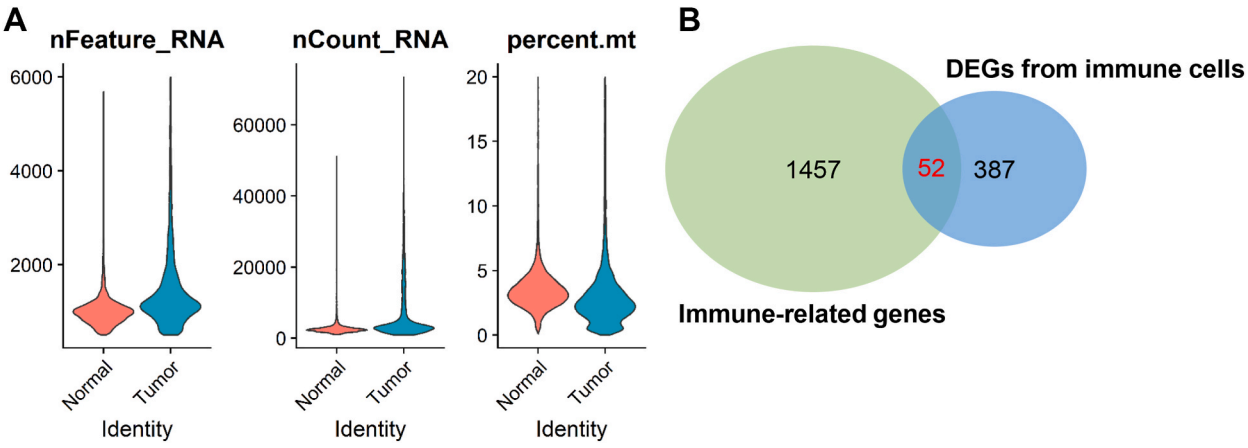

Fig. 2. Identification of IRDEGs. (A) Violin plots showing the quality control of scRNA-seq from GSE149614 dataset. (B) Venn diagram of the intersection between immune-related genes and differentially expressed genes in immune cells.

Table 1
The results of univariate cox regression analysis.

Univariate Cox regression analysis- significant genes	Hazard_Ratio	*P*-value
B2M	0.791021142	0.021823694
HSPA6	1.129316184	0.025203337
KNG1	0.897770135	0.000661572
PPIA	1.381698784	0.020353856
HRG	0.928755637	0.001775543
ACTG1	1.316656194	0.039810106

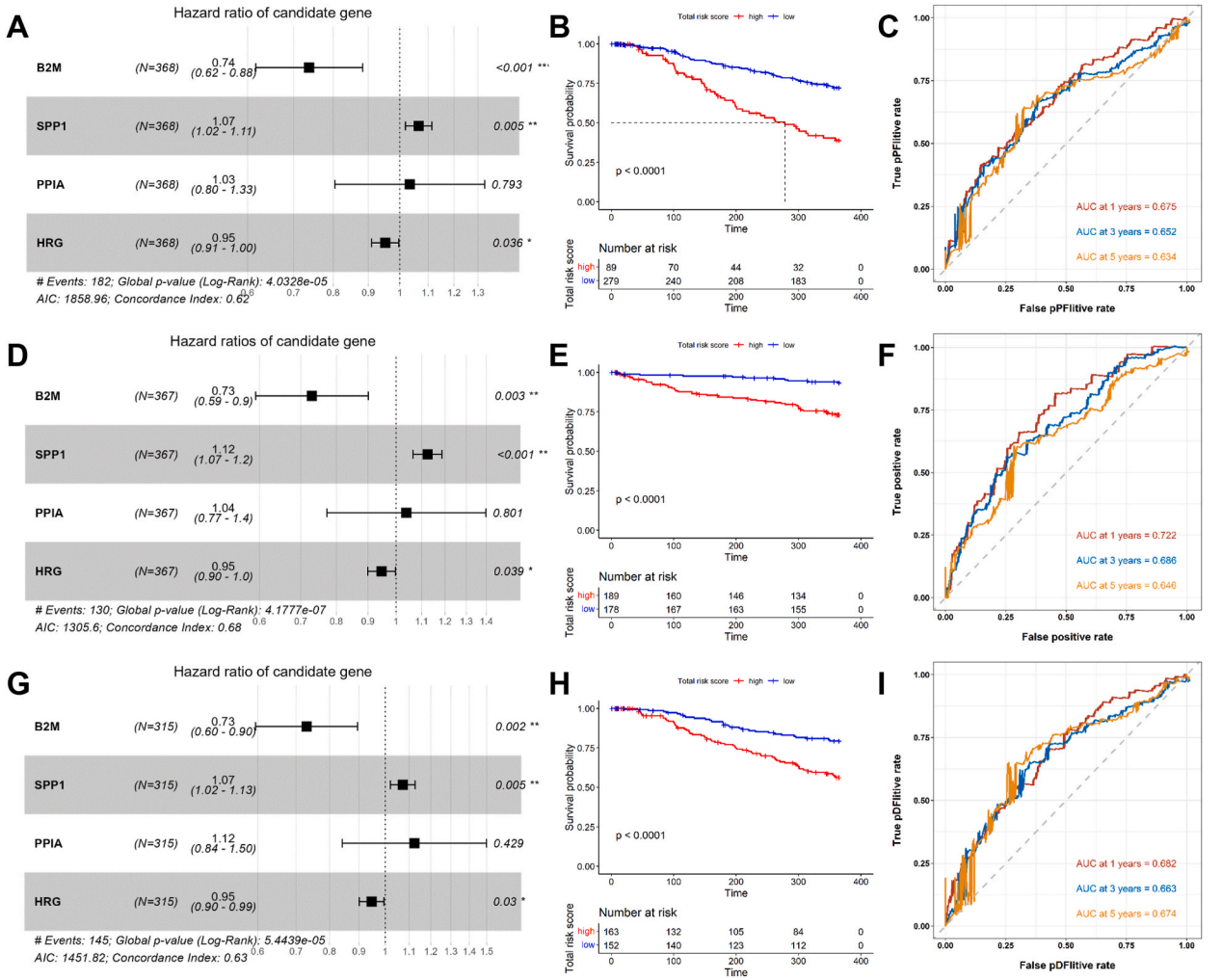

Fig. 3. Construction of immune-related prognostic model. Multivariate Cox analysis of PFI (A), OS (D), and DFI (G). K-M survival analysis of PFI (B), OS (E), and DFI (H). Time-dependent ROC curve analysis of PFI (C), OS (F), and DFI (I).

Sorafenib had no significant difference between high-risk group and low-risk group (Figs. S2B–F). These findings demonstrated that the risk model has the predictive ability in clinical treatment for HCC patients.

3.5. Validation of the risk model in the ICGC cohort and IRDEG expression in multiple cohorts and clinical specimens

The ICGC cohort was used to examine the accuracy of the prognostic model. In the ICGC cohort, K-M analysis showed that the low-risk group has better OS ($P < 0.0001$, Fig. 7A). The areas under the curve (AUCs) values at 1-, 3- and 5-year were 0.705, 0.749 and 0.667, respectively (Fig. 7B). We further evaluated the expressions of 4-IRDEGs in different datasets. In the TCGA-LIHC cohort and GSE54236 dataset, the expressions of B2M and HRG were down-regulated and the expressions of SPP1 and PPIA were up-regulated in tumor groups compared with the normal groups (Fig. 7C and D). In the GSE14520 dataset, the expressions of B2M, SPP1, and HRG

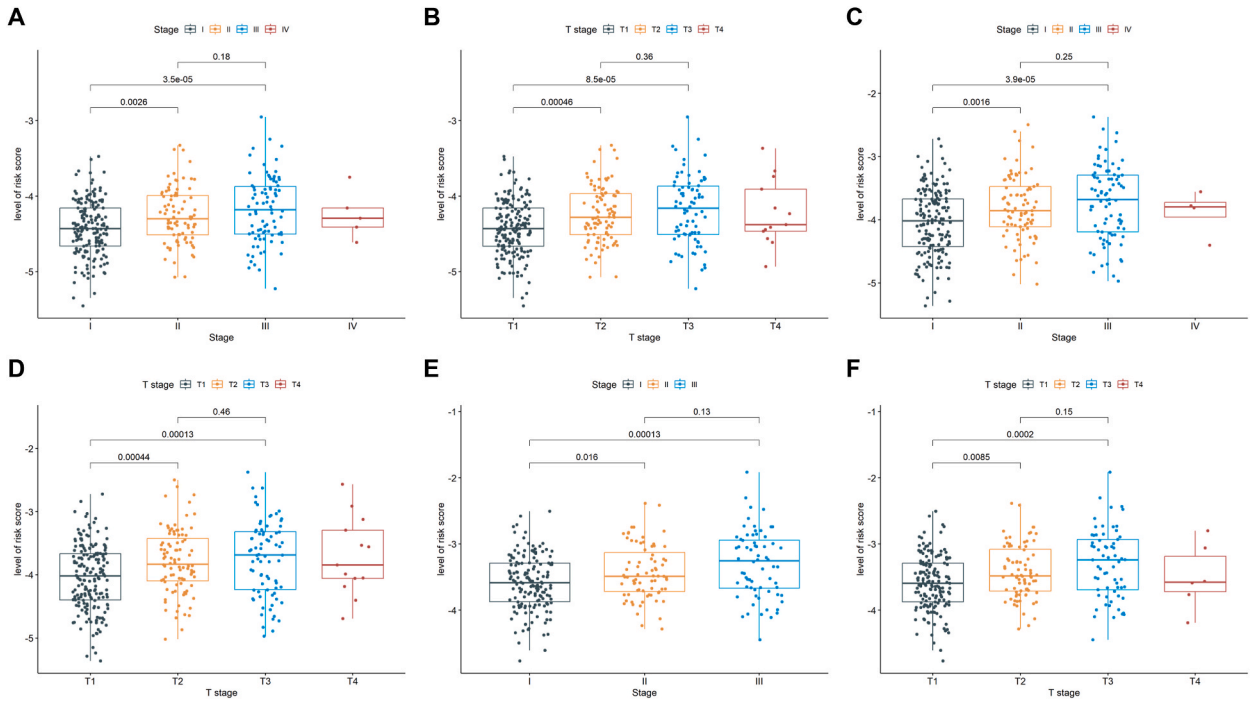

Fig. 4. The correlation between the prognostic model and the clinicopathological features. Advanced pathological stages of PFI (A), OS (C), and DFI (E). T stage of PFI (B), OS (D), and DFI (F).

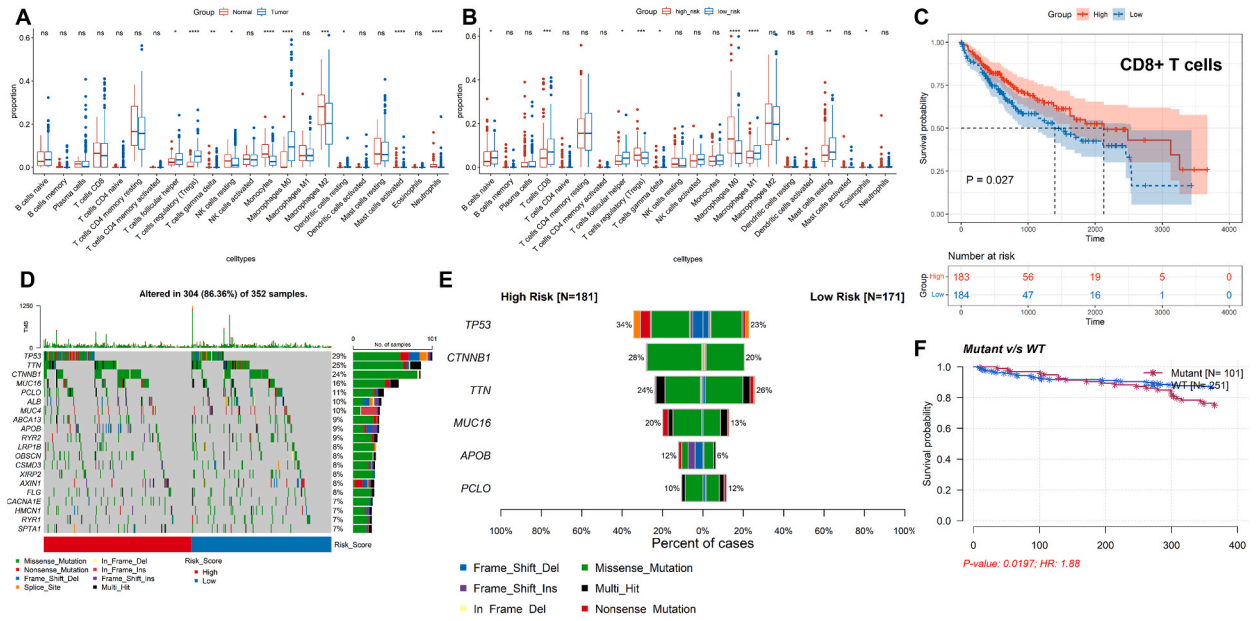

Fig. 5. Analyzing of potential immunotherapy-related signatures. (A) The Kruskal-Wallis test was used to compare the proportion of immune cells in normal and tumor samples. (*$P < 0.05$, ns indicated no significance). (B) The Kruskal-Wallis test was used to compare the proportion of immune cells in low-risk and high-risk groups. (*$P < 0.05$, ns indicated no significance). (C) K-M survival analysis of $CD8^+$ T cells. (D) The mutation profiles of the low- and high-risk groups. (E) Comparison of the mutation rate between low- and high-risk groups. (F) K-M survival analysis of mutation status of TP53.

were the same as the TCGA-LIHC cohort and GSE54236 dataset, while the expression of PPIA was declined in tumor group comparing to the normal group (Fig. 7E). Analogously, there was no significant difference in the expression of B2M between the two groups in the GSE64041 dataset, and the expression trend of other IRDEGs was consistent with the TCGA-LIHC cohort and GSE54236 dataset

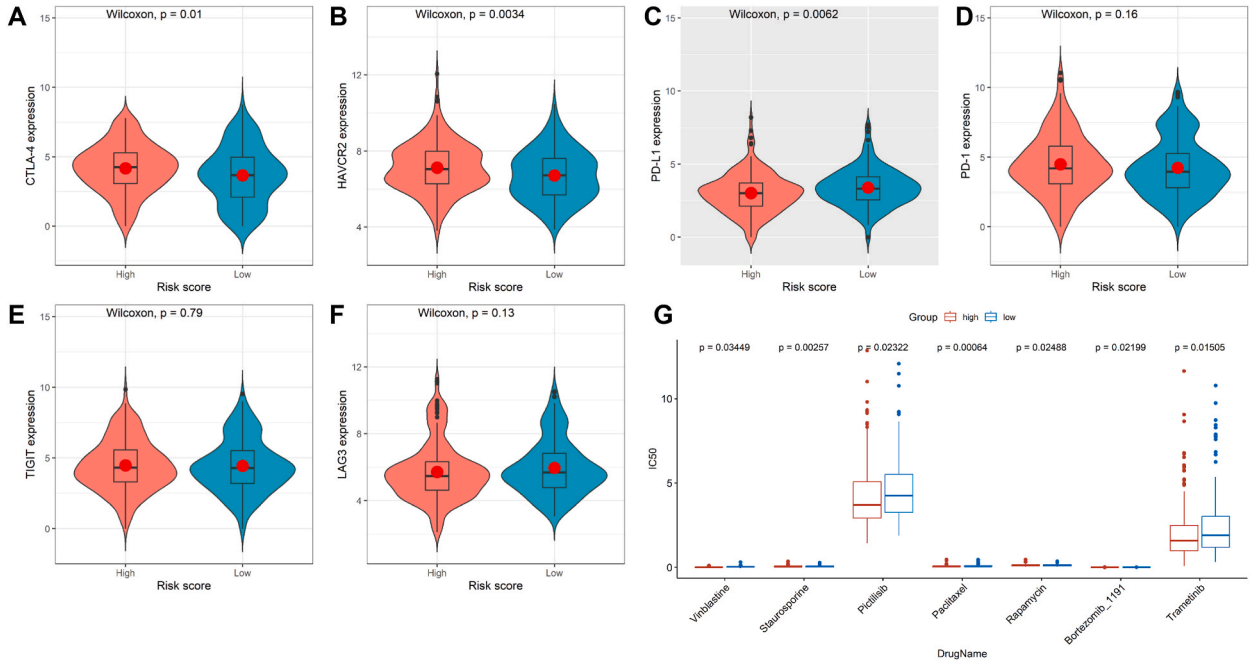

Fig. 6. Clinical treatment analysis of the risk model. Comparison of the expression of CTLA-4 (A), HAVCR2 (B), PD-L1 (C), PD-1 (D), TIGIT (E), and LAG3 (F) between low- and high-risk groups using Wilcoxon test. (G) The differences of estimated IC50 of 7 representative drugs between low- and high-risk groups.

(Fig. 7F). The q-PCR assay was performed to validate the expressions of 4-IRDEGs in clinical specimens. Compared with para-carcinoma tissues (normal group), the expressions of B2M and HRG in liver cancer were significantly down-regulated (Fig. 7G), while the expression of SPP1 was observably increased. PPIA had no significant difference in the two groups. These results indicated the risk model could accurately predict the prognosis of HCC patients, and the levels of IRDEGs was associated with the development of HCC.

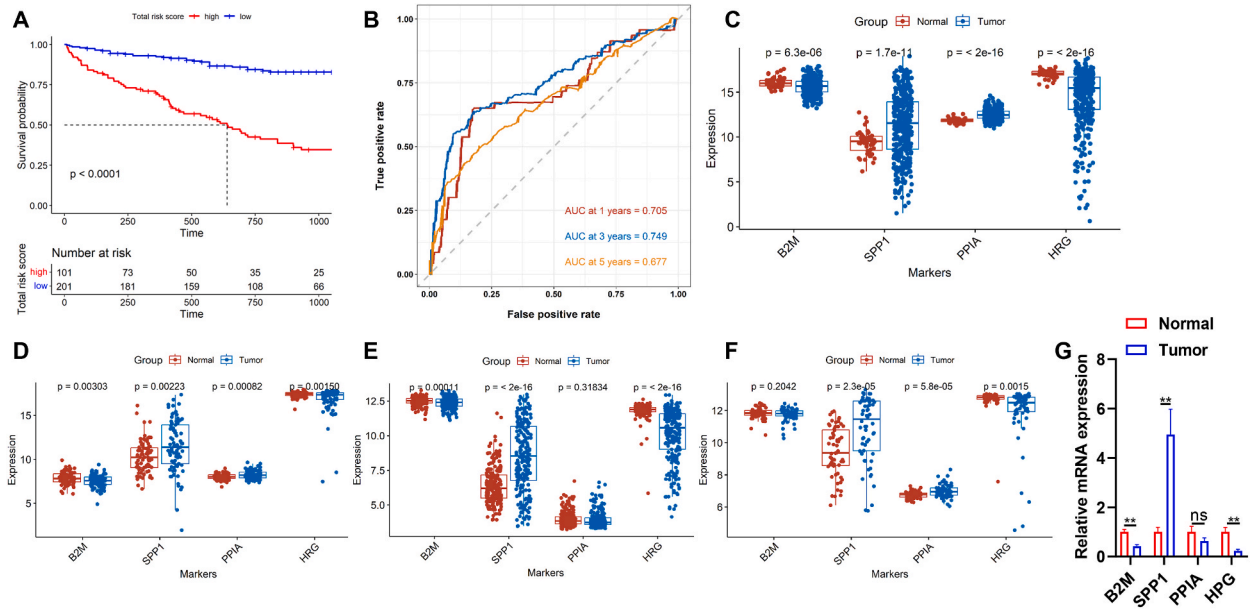

Fig. 7. Validation of the risk model in the ICGC cohort and 4-IRDEGs expression in multiple datasets and clinical samples. (A) K-M survival analysis of the ICGC cohort. (B) Time-dependent ROC curve analysis of the ICGC cohort. Comparison of 4-IRDEGs expression between tumor and normal samples in TCGA-LIHC cohort (C), GSE54236 (D), GSE14520 (E), and GSE64041 (F). (G) Clinical validation of 4-IRDEGs expression. (*$P < 0.05$, ns indicated no significance).

4. Discussion

Immunotherapy has become available therapy for HCC. However, due to the heterogeneity of the TME, the interaction of immune cells in TME not only affects the progression of the tumor, but also influences the effect of immunotherapy [23]. However, the role of TME and immune cells in HCC prognosis remains unclear. Therefore, it is urgent to explore new prognostic biomarkers from immune cells from TME that have the power to forecast the efficacy of immunotherapy and survival in HCC patients.

TME in HCC is associated with immune cell infiltration [24]. In this study, according to the scRNA-seq of HCC, we established a prognostic model based on 4-IRDEGs from immune cells and immune-related genes, which can predict the pathological stage and prognosis of HCC patients. Besides, the risk model could reflect the tumor immune microenvironment and somatic cell mutations, thereby providing references for clinical guidance for the treatment of HCC patients.

Our prognostic risk model was developed from 4-IRDEGs with prognostic significance, named B2M, SPP1, PPIA, and HRG. B2M, as an antigen presentation gene, its alteration effects the normal folding and transport of major histocompatibility complex (MHC) class I to the cell surface, resulting in resistance to immune checkpoint inhibitors [25,26]. Moreover, B2M mutations could cause impairment in the recognition of tumor antigens by CD8+T cells [27,28]. Liu et al. [29] reported that SPP1 could accelerate the polarization of macrophages to m2 phenotype tumor-related macrophages, thus promoting the occurrence and development of HCC. In addition, SPP1, as an anoikis-related rognostic gene, can efficiently predict the OS and tumor immune microenvironment of HCC [30]. PPIA is highly expressed in HCC and enhances the malignant phenotype of HCC cells [31]. Besides, PPIA with high expression promoted the resistance of HCC to sorafenib, which leads to poor prognosis of HCC [32]. Zhang et al. found that HRG was at a low level in HCC, and overexpression of HRG inhibited the proliferation and tumor formation of HCC cells [33]. The above studies have shown that the 4-IRDEGs are related to the immunotherapy and tumor progression of HCC, which is very important for predicting the prognosis and immune response of HCC.

To assess the clinical applicability of this prognostic model, we analyzed the correlation between the model and pathological stage. The higher risk score was positively related to pathological stage, which is consistent with other HCC prognostic models [34], confirming the reliability of our prognostic model. In addition, TME is important for regulating tumor progression and immune response in HCC. Furthermore, the risk scores were negatively related to the infiltration of naive B cells, $CD8^+$ T cells, follicular helper T cells, and M1 macrophages. Study has shown that B cell infiltration is positively correlated with the response of tumor patients to immunotherapy [35]. $CD8^+$ T cell responses are critical for anti-tumor immunity [36]. CD8+T cell depletion reduces the efficacy of anti-PD-1 therapy against HCC [37]. M1 macrophages are generally considered to be tumor-killing macrophages, mainly with anti-tumor and immune-promoting effects. Hao et al. [38] found that inhibition of APOC1 can promote the transformation of M2 macrophages into M1 macrophages, thereby reshaping the TME and improving the immunotherapy effect of anti-PD1 on HCC. These studies explained the poorer prognosis in high-risk populations in our risk model.

Somatic mutation can be an important index to predict the clinical efficacy of immunotherapy [39]. Our results showed that TP53 in the high-risk group was accompanied by a high mutation rate, while MUC16 with high mutation rate was in the low-risk group, which is consistent with other report [40]. Additionally, compared with the wild type, TP53 with high mutation rate has a poor prognosis in HCC patients, which may be related to the involvement of TP53 mutations in the occurrence and development of HCC [41]. Moreover, our prognostic model can predict HCC patients who will benefit from ICIs therapy and chemotherapy, which may improve guidance for personalized treatment of HCC.

5. Conclusion

In summary, IRDEG could be as an immune-related prognostic biomarker for HCC. Our prognostic model performed well in predicting the outcomes and immunotherapy of HCC patients, highlighting the understanding of the relationship between immune cells and TME.

Consent for publication

All the authors have provided consent for the publication.

Data availability statement

The datasets used in this study were all from public databases.

Ethics declarations

This study was reviewed and approved by the Ethics Committee of Third People's Hospital of Shenzhen (No. 2022-068). All participants provided written informed consent to participate in this study and for their data to be published. All experimental methods follow the guidelines established in the Helsinki Declaration.

Funding

This work was supported by the funds for the construction of key medical disciplines in Shenzhen (SZXK076).

CRediT authorship contribution statement

Lichao Cao: Writing – original draft, Formal analysis, Conceptualization. **Deliang Huang:** Writing – original draft, Formal analysis, Conceptualization. **Shenrui Zhang:** Formal analysis, Data curation. **Zhiwei Li:** Software, Methodology. **Qingxian Cai:** Resources, Data curation. **Fang Chen:** Validation, Methodology. **Meilan Zhu:** Visualization, Validation. **Ying Ba:** Methodology. **Jun Chen:** Writing – review & editing, Project administration, Conceptualization. **Hezi Zhang:** Writing – review & editing, Project administration, Conceptualization.

Declaration of competing interest

The authors declare that they have no known competing financial interests or personal relationships that could have appeared to influence the work reported in this paper.

Appendix A. Supplementary data

Supplementary data to this article can be found online at https://doi.org/10.1016/j.heliyon.2024.e34012.

References

[1] J.M. Llovet, R.K. Kelley, A. Villanueva, Hepatocellular carcinoma 7 (1) (2021) 6.
[2] L. Kulik, H.B. El-Serag, Epidemiology and management of hepatocellular carcinoma, Gastroenterology 156 (2) (2019) 477–491.e1.
[3] H. Rumgay, M. Arnold, J. Ferlay, O. Lesi, C.J. Cabasag, J. Vignat, et al., Global burden of primary liver cancer in 2020 and predictions to 2040, J. Hepatol. 77 (6) (2022) 1598–1606.
[4] J. Li, Y. Zhu, Recent advances in liver cancer stem cells: non-coding RNAs, oncogenes and oncoproteins, Front. Cell Dev. Biol. 8 (2020) 548335.
[5] D. Feng, M. Wang, J. Hu, S. Li, S. Zhao, H. Li, et al., Prognostic value of the albumin-bilirubin grade in patients with hepatocellular carcinoma and other liver diseases, Ann. Transl. Med. 8 (8) (2020) 553.
[6] C. Laface, G. Ranieri, F.M. Maselli, F. Ambrogio, C. Foti, M. Ammendola, Immunotherapy and the combination with targeted therapies for advanced hepatocellular carcinoma 15 (3) (2023).
[7] K. Oura, A. Morishita, The roles of epigenetic regulation and the tumor microenvironment in the mechanism of resistance to systemic therapy in hepatocellular carcinoma 24 (3) (2023).
[8] J.M. Keilson, H.M. Knochelmann, C.M. Paulos, R.R. Kudchadkar, M.C. Lowe, The evolving landscape of immunotherapy in solid tumors 123 (3) (2021) 798–806.
[9] A.B. El-Khoueiry, B. Sangro, T. Yau, T.S. Crocenzi, M. Kudo, C. Hsu, et al., Nivolumab in patients with advanced hepatocellular carcinoma (CheckMate 040): an open-label, non-comparative, phase 1/2 dose escalation and expansion trial, Lancet 389 (10088) (2017) 2492–2502.
[10] T. Yau, J.W. Park, R.S. Finn, A.L. Cheng, P. Mathurin, J. Edeline, et al., Nivolumab versus sorafenib in advanced hepatocellular carcinoma (CheckMate 459): a randomised, multicentre, open-label, phase 3 trial, Lancet Oncol. 23 (1) (2022) 77–90.
[11] A.T. Tan, S. Schreiber, Adoptive T-cell therapy for HBV-associated HCC and HBV infection, Antivir. Res. 176 (2020) 104748.
[12] X. Kong, Discovery of new immune checkpoints: family grows up, Adv. Exp. Med. Biol. 1248 (2020) 61–82.
[13] C. Chen, Z. Wang, Y. Ding, Y. Qin, Tumor microenvironment-mediated immune evasion in hepatocellular carcinoma, Front. Immunol. 14 (2023) 1133308.
[14] F. Baharom, R.A. Ramirez-Valdez, A. Khalilnezhad, S. Khalilnezhad, M. Dillon, D. Hermans, et al., Systemic vaccination induces CD8(+) T cells and remodels the tumor microenvironment, Cell 185 (23) (2022) 4317–4332.e15.
[15] J.A. Myers, J.S. Miller, Exploring the NK cell platform for cancer immunotherapy, Nat. Rev. Clin. Oncol. 18 (2) (2021) 85–100.
[16] O. Kyrysyuk, K.W. Wucherpfennig, Designing cancer immunotherapies that engage T cells and NK cells, Annu. Rev. Immunol. 41 (2023) 17–38.
[17] R. Cabrita, M. Lauss, A. Sanna, M. Donia, M. Skaarup Larsen, S. Mitra, et al., Tertiary lymphoid structures improve immunotherapy and survival in melanoma, Nature 577 (7791) (2020) 561–565.
[18] Y. Lu, A. Yang, C. Quan, Y. Pan, A single-cell atlas of the multicellular ecosystem of primary and metastatic hepatocellular carcinoma 13 (1) (2022) 4594.
[19] L. Cao, S. Zhang, D. Yao, Y. Ba, Q. Weng, J. Yang, et al., Comparative analyses of the prognosis, tumor immune microenvironment, and drug treatment response between left-sided and right-sided colon cancer by integrating scRNA-seq and bulk RNA-seq data, Aging (Albany NY) 15 (14) (2023) 7098–7123.
[20] A.M. Newman, C.L. Liu, M.R. Green, A.J. Gentles, W. Feng, Y. Xu, et al., Robust enumeration of cell subsets from tissue expression profiles, Nat. Methods 12 (5) (2015) 453–457.
[21] A. Mayakonda, D.C. Lin, Y. Assenov, C. Plass, H.P. Koeffler, Maftools: efficient and comprehensive analysis of somatic variants in cancer, Genome Res. 28 (11) (2018) 1747–1756.
[22] D. Maeser, R.F. Gruener, R.S. Huang, oncoPredict: an R package for predicting in vivo or cancer patient drug response and biomarkers from cell line screening data, Briefings Bioinf. 22 (6) (2021).
[23] D. Bruni, H.K. Angell, J. Galon, The immune contexture and Immunoscore in cancer prognosis and therapeutic efficacy, Nat. Rev. Cancer 20 (11) (2020) 662–680.
[24] Y. Chen, Y. Zhou, Z. Yan, P. Tong, Q. Xia, K. He, Effect of infiltrating immune cells in tumor microenvironment on metastasis of hepatocellular carcinoma, Cell. Oncol. 46 (6) (2023) 1595–1604.
[25] H. Wang, B. Liu, J. Wei, Beta2-microglobulin(B2M) in cancer immunotherapies: biological function, resistance and remedy, Cancer Lett. 517 (2021) 96–104.
[26] J.M. Zaretsky, A. Garcia-Diaz, D.S. Shin, H. Escuin-Ordinas, W. Hugo, S. Hu-Lieskovan, et al., Mutations associated with acquired resistance to PD-1 blockade in melanoma, N. Engl. J. Med. 375 (9) (2016) 819–829.
[27] C.E. Rudd, CD8+ T cell killing of MHC class I–deficient tumors, Nat. Can. (Ott.) 4 (9) (2023) 1214–1216.
[28] H. Zhang, B. Cui, Y. Zhou, X. Wang, W. Wu, Z. Wang, et al., B2M overexpression correlates with malignancy and immune signatures in human gliomas, Sci. Rep. 11 (1) (2021) 5045.
[29] L. Liu, R. Zhang, J. Deng, X. Dai, X. Zhu, Q. Fu, et al., Construction of TME and Identification of crosstalk between malignant cells and macrophages by SPP1 in hepatocellular carcinoma 71 (1) (2022) 121–136.
[30] Y. Chen, W. Huang, J. Ouyang, J. Wang, Z. Xie, Identification of anoikis-related subgroups and prognosis model in liver hepatocellular carcinoma 24 (3) (2023).
[31] S. Cheng, M. Luo, C. Ding, C. Peng, Z. Lv, R. Tong, et al., Downregulation of Peptidylprolyl isomerase A promotes cell death and enhances doxorubicin-induced apoptosis in hepatocellular carcinoma, Gene 591 (1) (2016) 236–244.
[32] L. Li, S. Yu, J. Chen, M. Quan, Y. Gao, miR-15a and miR-20b sensitize hepatocellular carcinoma cells to sorafenib through repressing CDC37L1 and consequent PPIA downregulation 8 (1) (2022) 297.

[33] Q. Zhang, K. Jiang, Y. Li, D. Gao, L. Sun, S. Zhang, et al., Histidine-rich glycoprotein function in hepatocellular carcinoma depends on its N-glycosylation status, and it regulates cell proliferation by inhibiting Erk1/2 phosphorylation, Oncotarget 6 (30) (2015) 30222–30231.
[34] G. Zhang, J. Sun, X. Zhang, A novel Cuproptosis-related LncRNA signature to predict prognosis in hepatocellular carcinoma, Sci. Rep. 12 (1) (2022) 11325.
[35] B.A. Helmink, S.M. Reddy, J. Gao, S. Zhang, R. Basar, R. Thakur, et al., B cells and tertiary lymphoid structures promote immunotherapy response, Nature 577 (7791) (2020) 549–555.
[36] M.K. Rahim, T.L.H. Okholm, K.B. Jones, E.E. McCarthy, C.C. Liu, J.L. Yee, et al., Dynamic CD8(+) T cell responses to cancer immunotherapy in human regional lymph nodes are disrupted in metastatic lymph nodes, Cell 186 (6) (2023) 1127–1143.e18.
[37] X. Zhang, Z. Wei, T. Yong, Cell microparticles loaded with tumor antigen and resiquimod reprogram tumor-associated macrophages and promote stem-like CD8(+) T cells to boost anti-PD-1 therapy 14 (1) (2023) 5653.
[38] X. Hao, Z. Zheng, H. Liu, Y. Zhang, J. Kang, X. Kong, et al., Inhibition of APOC1 promotes the transformation of M2 into M1 macrophages via the ferroptosis pathway and enhances anti-PD1 immunotherapy in hepatocellular carcinoma based on single-cell RNA sequencing, Redox Biol. 56 (2022) 102463.
[39] J. Douglass, E.H. Hsiue, Bispecific antibodies targeting mutant RAS neoantigens 6 (57) (2021).
[40] Z. Wu, Z. Lu, L. Li, M. Ma, F. Long, R. Wu, et al., Identification and validation of ferroptosis-related LncRNA signatures as a novel prognostic model for colon cancer, Front. Immunol. 12 (2021) 783362.
[41] Y. Zhou, G. Cui, H. Xu, J. Chun, D. Yang, Z. Zhang, et al., Loss of TP53 cooperates with c-MET overexpression to drive hepatocarcinogenesis 14 (7) (2023) 476.